Turbines' effects on water renewal within a marine tidal stream energy site

Nicolas Guillou, Jérôme Thiebot, Georges Chapalain

Version of Record: https://www.sciencedirect.com/science/article/pii/S0360544219318080
Manuscript_a756c5aff191fd8452bee1bd2a84e837

Turbines' effects on water renewal within a marine tidal stream energy site

Nicolas Guillou[a,*], Jérôme Thiébot[b], Georges Chapalain[a]

[a] *Cerema, Direction Eau Mer et Fleuves, Environnement et Risques, Laboratoire de Génie Côtier et Environnement (LGCE), 155 rue Pierre Bouguer, Technopôle Brest-Iroise, BP 5, 29280, Plouzané, France*
[b] *Normandie University, UNICAEN, LUSAC, EA4253, site universitaire de Cherbourg, rue Louis Aragon, BP 78, F-50130, Cherbourg-Octeville, France*

Abstract

As tidal stream energy sites contribute to a significant part of water transport in coastal shelf seas, turbines' implementation may lead to system-wide changes of the hydrodynamic circulation with potential effects on marine water quality. These aspects were investigated in north-western coastal waters of Brittany (France, western Europe) by simulating the decay of a tracer concentration within a control domain surrounding the tidal stream energy site of the Fromveur Strait. Simplified simulations were adopted to analyse the sensitivity of tracer distribution to stream energy extraction. While this marine area showed important renewal capacity with a 50% loss of tracer concentration in less than three days, residual values were still present after two months. This result exhibited that the concentration decay could not be calibrated by simple exponential functions. The renewal of marine waters appeared furthermore dependent on tracer release time during a tidal cy-

*Corresponding author
Email address: nicolas.guillou@cerema.fr (Nicolas Guillou)

cle. A full energy-extraction scenario was finally simulated suggesting weak effects of turbines on the renewal capacity with changes in residence times below 5%. The spatio-temporal Eulerian evolution of the concentration revealed, however, local trapping areas in close correlation with the Lagrangian residual circulation that vanished after two months.
Keywords: marine water quality; tidal stream energy extraction; Fromveur Strait; Ushant-Molène archipelago; Brittany; Telemac.

1. Introduction

As a highly predictable renewable resource with reduced visual impacts of energy converters, the hydro-kinetic power of tidal currents has attracted, during the last decade, the interest of governments that committed to reduce carbon dioxide emissions. Tidal stream energy converters are still in the early stages of development with limited investments to support the emergence of next-generation disruptive technologies viable for a massive exploitation of the resource [1]. However, existing devices such as horizontal-axis turbines appear yet as a promising solution to supply a part of sustainable fossil-free resource within energy-starved territories or areas unconnected to the continental electricity grid, such as islands systems [2].

Successful deployments and operations of turbines array within these environments require refined assessments of the potential environmental and ecological impacts of increased energy-extraction scenarios, assessing in particular the effects on the quality of marine waters. Indeed, as tidal stream energy sites contribute to significant transport of water in estuarine and coastal marine systems, operating turbines arrays may lead to system-wide

changes of the hydrodynamic circulation and water-particles displacement. This includes modifications in trapping and dispersion of dissolved nutriments and pollutants (e.g., oil, persistent toxins), particulate organic matters (e.g., plankton, gametes, larvae) and sediments [3, 4, 5]. Large-scale effects on biochemical processes such as renewal of dissolved oxygen or primary production are also expected [6, 7].

The few numerical studies about water-quality changes originally focused on tidal channels that connect a bay or an estuary to the coastal ocean (see [8] for a review). Simulations computed the spatio-temporal distribution of a conservative tracer and evaluated (i) the times required for the removal of fresh waters within these environments and (ii) the variations induced by energy extraction within tidal channels [9, 10, 11]. The ecological robustness of marine systems was found to vary significantly with respect to (i) the stream-energy site, (ii) the extraction scenario and (iii) the numerical model considered. In an idealised channel linked to a bay, Yang et al. [9] reported that a small variation of 15% in the volume flux through turbines farms was leading to changes of 100% in the bay flushing time. Such a strong disturbance was simulated by Nash et al. [10] in the Shannon estuary (Ireland) with an increase of the average residence time of water up to 70% for a high density farms. Wang and Yang [11] obtained, however, weak differences in water residence time by extracting tidal-stream energy from minor channels within the multi-inlet bay system of Puget Sound (USA).

Complementing these investigations restricted to bays and estuaries, numerical models were applied to tidal stream energy sites in continental shelf ecosystems. Shapiro [12] computed the effects of a turbine array on drifters

transport in the Celtic Sea (UK, north of Cornwall) exhibiting significant changes, up to 238%, in the travelling distance of floats. Van der Molen et al. [6] and De Dominicis et al. [7] assessed the large-scale effects of energy extraction within the Pentland Firth (UK, north of Scotland) on seasonal stratification and biogeochemical processes, reporting variations over hundred of kilometres away from the turbines farm for a massive-expansion scenario. More recently, Guillou and Chapalain [13, 14] evaluated the effects of a series of turbines arrays within the Fromveur Strait (France, western Brittany, Fig. 1) suggesting changes in (i) the magnitude and direction of the residual Lagrangian circulation emerging from the strait and (ii) the locations of surrounding eddies (Fig. 2). However, unlike tidal bays and estuaries, little effort was devoted to the effects of turbines array on the renewal of marine waters in the coastal ocean.

The present study complements these numerical investigations by assessing the effects of tidal stream energy extraction on the renewal of marine waters within the Ushant-Molène archipelago and the Fromveur Strait (Section 2). This investigation provides furthermore a preliminary assessment of the renewal capacity of this marine area and its resilience to turbines' induced perturbations. Following simulations conducted on water renewals in bays and estuaries [9, 10, 11], the approach, adopted here, relied on a high-resolution depth-averaged tidal circulation model that simulated the spatio-temporal distribution of a tracer concentration initially released within the marine environment (Sections 3.1 and 3.2). Tide was assumed as the dominant hydrodynamic forcing neglecting the contributions of wind, waves and thermal fronts. The renewal capacity of the Ushant-Molène archipelago was

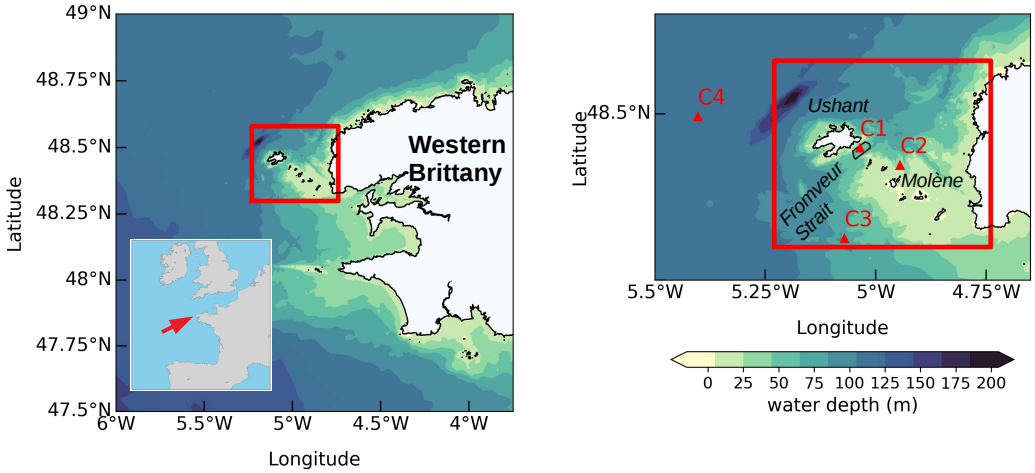

Figure 1: Overview of the bathymetry in western Brittany with a detailed view within the Ushant-Molène archipelago. Water depth is relative to mean sea level. The locations of available measurement points are indicated with red triangles. The red line circumscribes the control domain where an unity tracer concentration is initially prescribed. The black line delimits the area of interest for the implementation of turbines within the Fromveur Strait.

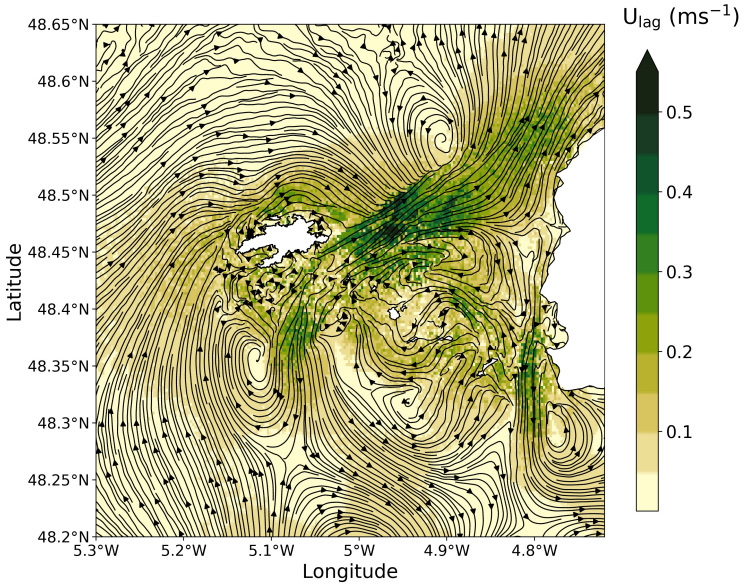

Figure 2: Streamlines from M_2 tidal residual Lagrangian currents within the Ushant-Molène archipelago [adapted from 13].

estimated by simulating the spatio-temporal evolution of the tracer concentration in the area of interest. Following numerical impact studies of tidal stream energy extraction [15, 16, 17, 18], the hydrodynamic disturbances induced by devices were simulated as an equivalent drag form term redistributing the sum of turbines' thrust over the area covered by the proposed array (Section 3.3). This simplified numerical approach contrasted with more complex three-dimensional simulations (i) routinely implemented in resource assessments [19, 20, 21] and (ii) with advanced representation of individual turbines [22, 23]. However, these more advanced simulations required important computational costs that reduced applications to short period of time and limited spatial coverage (typically the scale of the tidal-farm array). Our hydrodynamic predictions were assessed against available measurements of current amplitude and direction at four locations in the area of interest (Section 4.1). Particular attention was dedicated to the sensitivity of water-renewal predictions to the release time of tracer concentration at the semi-diurnal and spring-neap time scales (Section 4.2). We finally evaluated the effects of a full energy-extraction scenario on the renewal capacity of the archipelago and the spatio-temporal distribution of tracer concentration (Section 4.3).

2. Study area

Located at the western extend of Brittany, the Fromveur Strait separates the island of Ushant from a series of islets and rocks that form the Molène archipelago (Fig. 1). This 2 km wide and 50 m deep strait is characterised, after the Alderney Race in the English Channel, by the second

largest tidal currents along the coast of France with peak velocities exceeding 4 $\mathrm{m\,s^{-1}}$ [24, 25]. The available tidal stream power density may furthermore reach values over 20 $\mathrm{kW\,m^{-2}}$ in mean spring conditions at 10 m above the seabed, the hub height of planned horizontal-axis turbines for this region [18, 26]. Considering this prominent energy resource, the French government has identified a restricted area of 4 $\mathrm{km^2}$ within the strait for the development of tidal farm projects. Following this roadmap, the company Sabella SAS is conducting the optimisation process of a turbine with a diameter of 10 m to supply a part of electricity to the Ushant grid [27]. This marine ecosystem is also an emblematic area of western Brittany integrated, since 1988, in the Iroise biosphere reserve by Unesco with high environmental constraints to guarantee water quality standards and biodiversity preservation. It is thus fundamental to gain further insights about the potential environmental impacts of operating turbines within this area.

Numerical studies conducted within this coastal environment mainly examined (i) the available tidal-stream power resource and (ii) the potential large-scale environmental effects of energy extraction setting aside further investigations about changes induced on water transport and tracer dispersals [18, 25, 26, 28]. Guillou and Chapalain [13, 14] evaluated, however, the tide-induced Lagrangian circulation in idealised conditions driven by the principal lunar semi-diurnal component $\mathrm{M_2}$. The residual circulation exhibited a central divergence area within the Fromveur Strait between (i) a prominent north-eastern pathway with currents up to 0.45 $\mathrm{m\,s^{-1}}$ and (ii) a southward circulation (Fig. 2). This central divergence pattern resulted from (i) a northern area characterised by northeast-directed flood-dominated

flows, and (ii) a southern area experiencing southward ebb-dominated currents [13, 18, 25]. This major Lagrangian feature was bordered by prominent cyclonic and anti-cyclonic recirculations, with diameters of around 8 km, both upstream and downstream the strait. The extraction of tidal stream energy within the strait was found to impact the hydrodynamic circulation up to 15 km from the turbines array. Operating turbines modified thus the amplitude and direction of residual currents along the north-eastern and southward pathways emerging from the strait. Energy extraction impacted furthermore the locations of surrounding eddies that moved closer to the tidal stream energy site as the number of turbines increased within the farm. Further effects were thus expected on the renewal on marine waters at the scale of the Ushant-Molène archipelago.

3. Method

3.1. Hydrodynamic simulations

Simulations were conducted with the bi-dimensional horizontal model Telemac 2D (version v7p2r2) [29], by relying on the implementation performed by Guillou and Chapalain [21] in western Brittany. The model resolves the shallow water Barré de Saint-Venant equations of continuity and momentum on a planar unstructured computational grid with refined spatial resolutions in areas of interest. This unstructured grid offers thus the possibility to deal with the complexity of the shoreline topography around headlands and shoals of prominent importance for the spatial distribution of tidal circulation patterns [13]. The computational grid was composed of 51,226 nodes with a spatial resolution of around 10 km at offshore sea boundaries

to 50 m within the Fromveur Strait. The time step was set to 1 s. The horizontal momentum diffusion coefficient (eddy viscosity) was computed with a depth-averaged turbulence $k - \epsilon$ model. Assuming logarithmic vertical velocity profiles, the bottom shear stress was approached with a quadratic friction law parametrised with the roughness parameter z_0, defined as the height above the seabed at which the fluid velocity was set to zero. Considering hydrodynamically rough turbulent regimes, z_0 was formulated in terms of physical roughness of the bed neglecting the influences of water viscosity and current speed [18]. Following Guillou and Thiébot [18], its value was determined by matching sediment bottom types mapped by Hamdi et al. [30] with bottom roughness observations compiled by Soulby [31]. A value of $z_0 = 20$ mm was furthermore retained over rock outcrops.

The north-western coastal waters of Brittany were subjected to strong incoming waves [32, 33] and noticeable wave and current interactions [28]. Wind-generated surface-gravity waves may thus influence tidal currents and the associated stream energy resource [34]. Nevertheless, in the strait, these effects were mainly exhibited in storm conditions (with offshore wave height over 5 m) [26]. In spite of spring and summer density stratification effects resulting from the generation of offshore and nearshore thermal fronts [35, 36], minimal density effects were furthermore expected in the tidally-mixed waters of the Fromveur Strait. Simulations disregarded these effects restricting the investigation to the dominant tidal circulation.

The model was thus driven by harmonic tidal components of the TPXO8-atlas database covering the area of interest with a spatial resolution of $1/30^{\circ}$ [37]. The number of tidal components, used to drive the numerical model, dif-

fered between validation simulations and tracer transport predictions. Model performance was assessed against available current measurements by driving simulations with 13 major harmonic tidal components (K_1, O_1, P_1, Q_1, M_2, S_2, N_2, K_2, M_4, MS_4, MN_4, M_m and M_f) (Section 4.1). However, to be consistent with previous investigations on Lagrangian circulation pathways in the area of interest [13, 14], idealised tidal forcings were considered in tracer concentration simulations restricting the tidal recomposition to three harmonic components: the principal lunar M_2 and solar S_2 semi-diurnal harmonic constituents, and the first quarter-diurnal harmonic M_4 (Section 3.2). The harmonic M_4 was retained as the asymmetry in tidal currents within the Fromveur Strait arised from the phase relationship between M_2 and M_4 [13, 25]. This simplified tidal recomposition allowed furthermore a detailed investigation of the sensitivity of model results to the release time period of tracer concentration during a tidal cycle setting aside further variations associated with an increased number of harmonic components.

The evaluations of model predictions with respect to current observations were based on a series of statistical parameters including the Normalised Root-Mean-Square Error NRMSE $= \sqrt{1/n \sum_{i=1}^{i=n} (y_i - x_i)^2}/\bar{x}$, the Pearson's correlation coefficient R and the mean relative difference $\text{DIFF}_{rel} = 1/n \sum_{i=1}^{i=n}(y_i - x_i)$. n is the number of data in the discretised series considered, $\bar{x}$ is the mean value of observed data, and (x_i) and (y_i) represent the two sets of observed and simulated data, respectively. DIFF_{rel} was considered as an indicator of the tendency of the numerical model to over or underestimate available observations.

3.2. Water renewal study

3.2.1. Tracer transport simulations

Following numerical assessments of water exchanges in coastal bays and estuaries [38, 39, 40], the renewal of marine waters was estimated by simulating the evolution of a non-buoyant tracer concentration initially prescribed at an uniform unity value within a control domain surrounding the Ushant-Molène archipelago, between longitudes 5.23° W and 4.74°W, and latitudes 48.30°N and 48.58°N (Fig. 1). Preliminary numerical simulations confirmed the reduced sensitivity of the relative tracer concentration decay to the initial prescribed value. The initial tracer concentration was released in areas with mean water depths over 5 m to limit biases associated with water transport over tidal flats. The solute transport processes were computed with a depth-averaged advection-diffusion equation coupled with the hydrodynamic model (Section 3.1). The transport equation was thus resolved on the hydrodynamic computational grid with a time step of 1 s. The tracer diffusion coefficient was furthermore computed with the depth-averaged turbulence $k - \epsilon$ model [29]. This coefficient was, however, found to have negligible effects on tracer concentration simulations in the area of interest.

Particular attention was dedicated to the sensitivity of model predictions to the tidal phase of initial tracer releasing over semi-diurnal and spring-neap time scales (Fig. 3). Indeed, significant effects were expected as the initial mass of material was varying with water height and tidal range during the release time period. To be concordant with the water transport study of Guillou and Chapalain [13], a first series of simulations was thus performed in idealised periodic tidal conditions driving the numerical model by the

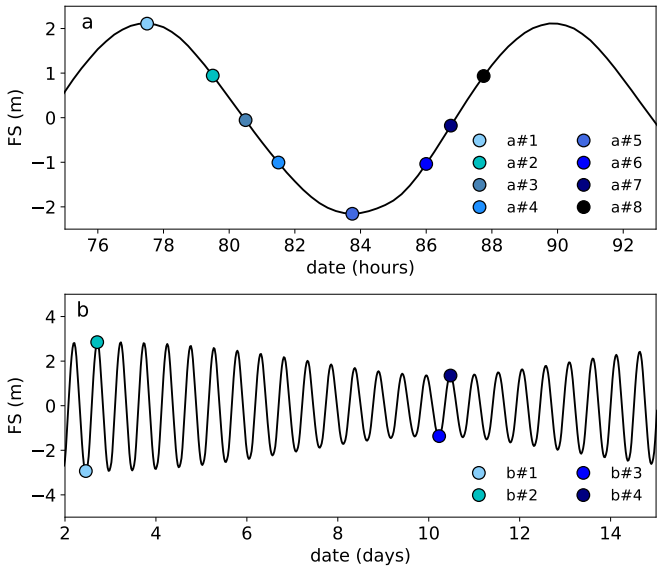

Figure 3: Time series of free-surface (FS) elevation in the center of the Fromveur Strait during (a) a M_2 tidal cycle and (b) a spring-neap tidal cycle resulting from M_2, S_2 and M_4 compound tides. The color circles denote the initial times when tracer concentration was released within the control domain surrounding the Ushant-Molène archipelago for simulations (i) #a1 to #a8 driving the model by M_2 and M_4, and (ii) #b1 to #b4 driving the model by M_2, S_2 and M_4.

principal lunar semi-diurnal harmonic component M_2 and its quarter-diurnal generated harmonic M_4. As inferred in numerical investigations conducted within the north-western European shelf seas [41, 42], the inclusion of M_4 harmonic in tidal forcing was found to improve its generation from M_2, especially in shallow waters close to open sea boundaries. These simulations, entitled a#1 to a#8, were conducted by releasing the tracer concentration at eight moments of a semi-diurnal tidal cycle (in high and low tides, during and in the vicinity of ebb and flood). A second series of simulations, entitled b#1 to b#4, complemented this simplified tidal forcing by considering

tracer releases in spring-neap tidal conditions resulting from M_2, S_2 and M_4 compound tides. In all simulations, the tidal hydrodynamic model was run during a minimum period of two days before prescribing the tracer concentration within the control domain, and predictions of tracer concentration were exploited with a time step of 30 min. Changes in trapping and dispersion of water were exhibited by (i) displaying the spatial distribution of tracer concentration at different time intervals during the simulation period, and (ii) evaluating the evolution of water renewal times within the control domain (defined in the next Section 3.2.2).

3.2.2. Water renewal times

In estuaries and multi-inlet bay systems, the retention and renewal of water are commonly evaluated by a variety of transport time descriptors, including, among the most used, the residence and flushing times, and the water age [43]. While these indicators were mainly considered in semi-enclosed coastal basins [e.g., 39, 40, 44, 45], numerical applications were also conducted in shelf environments such as the Irish Sea [38, 46] or the Liverpool Bay (UK) [47]. However, practical applications of these descriptors within marine areas require a refined definition of the underlying assumption and deviations between the idealised configuration and the real water bodies [40, 48, 49]. Transport time scales are typically evaluated with numerical modelling tools relying on (i) a Lagrangian procedure with particle tracking method or on (ii) an Eulerian framework with an advection-diffusion resolution of tracer concentration. For depth-averaged computations, the first approach is representative of a transport of pollutants at the sea surface whereas the second approach provides further information about concentration fluxes and wa-

ter transport (integrated along the water depth). The second method was thus adopted as the Ushant-Molène archipelago was characterised by strong tidal ranges. Nevertheless, the estimation of water renewal times with this method requires to follow the tracer concentration until it becomes negligible within the control domain. As these simulations involve extremely long computational time, simplified models based on exponential laws are proposed to approximate the concentration decay and handle the assessment of transport time scales. Following this assumption, the flushing time that defines the general exchange and renewal characteristics of a water body is estimated as the time required to replace (1-1/e) of the initial water in the area of interest by new water [50, 51]. This single ratio may, however, be irrelevant to account for the long-term evolution of tracer concentration, especially in cases when the decay differs from an exponential evolution [40] (Fig. 4). Taking into account these uncertainties, the renewal time of marine water was estimated as the durations required for the averaged concentration within the control domain to decrease by a series of percentiles from the initial concentration: 50, 30, 10 and 2%, respectively. The 2% value was retained to account for residual concentration values within the marine areas.

3.3. Tidal stream energy extraction

Tidal farm effects were included, at the scale of the 4 km^2 area within the Fromveur Strait (Fig. 1), as an additional bed friction sink term in the momentum equations of the tidal circulation model (Section 3.1). Following most numerical evaluations of the far-field environmental effects of a turbine array [15, 16, 17, 18], this sink term was determined by averaging the turbines' thrust forces over the area covered by the proposed array. The

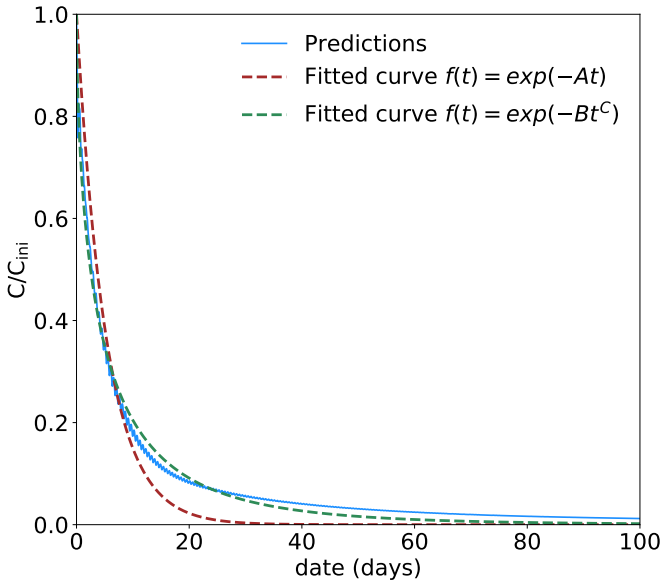

Figure 4: An example of times series of predicted relative concentration and regression curves fitted with (a) a simple exponential model ($f(t) = exp(-At)$) and (b) the exponential model of Murakami [52] ($f(t) = exp(-Bt^C)$). Whereas the second model provides a refined approach of predictions, it tends to overestimate the tracer concentration decay leading to biases in the estimation of transport time descriptors.

individual thrust force was computed as $F_T = \frac{1}{2}\rho C_t A|u|\vec{u}$ with A the area swept by turbine's blades, $\vec{u}$ the horizontal velocity component, ρ the water density taken equal to $\rho = 1025\,\mathrm{kg\,m^{-3}}$ and C_t the thrust coefficient set to $C_t = 0.8$ following Fernandez-Rodriguez et al. [53] and Frost et al. [54]. In the present investigation, fixed horizontal-axis turbines with a blade diameter of 15 m were considered according to future technologies for this region [55]. More complex formulations of the thrust forces were proposed introducing (i) a cut-in speed from which the turbine operates and (ii) a design speed at which device reaches its maximum rated power [16]. In order to

investigate the effects of tidal stream energy extraction, simpler formulations were, however, adopted modulating the extracted energy with the number of turbines within the array. Turbulence generated by operating devices was furthermore ignored. Indeed, as exhibited in the introduction, these aspects require refined three-dimensional modelling of individual devices with important computational costs to simulate the evolution of tracer concentration. Further details about the mathematical expressions and the numerical resolution adopted in Telemac 2D are available in Thiébot et al. [17] and Guillou and Thiébot [18].

4. Results and discussion

4.1. Evaluation of model predictions

Hydrodynamic model predictions were evaluated by comparison with in-situ observations of current amplitude and direction, provided by the French Navy SHOM ("Service Hydrographique et Océanographique de la Marine"), at four locations within the area of interest (Fig. 1 and Tab. 1). Further details about the instrumentation systems are available in Guillou and Thiébot [18]. Assuming vertical logarithmic velocity profiles, these comparisons were conducted in mid-water depths (Fig. 5). This evaluation extends, in particular, the assessment conducted by Guillou and Chapalain [13] restricted to the Fromveur Strait (point C1) and north of Molène (point C2) by including two locations in offshore waters, (i) south of the archipelago (point C3) and (ii) west of Ushant (point C4). The main difference with respect to previous numerical investigations lies furthermore in the spatial resolution of the tidal harmonic database used to drive simulations, of 1/4° for

Guillou and Thiébot [18], 1/12° for Guillou and Chapalain [13] and 1/30° in the present modelling. However, the implementation of a tidal harmonic database with a refined spatial resolution resulted in negligible improvements of numerical predictions at points C1 and C2. For the three numerical configurations, the hydrodynamic model reproduced thus the observations within the Fromveur Strait (point C1), approaching (i) the weak currents asymmetry characterised by slightly larger amplitude during south-western ebb and (ii) the abrupt changes between south-west and north-east directions. Whereas increased differences were obtained to the north of Molène in relation to complex hydrodynamics recirculations impacted by shoals and islands (Tab. 2), predictions approached also the observed time series of current amplitude and direction. The simulation reproduced thus, in this location, the observed (i) short north-eastern components and (ii) slightly reduced, long-lasting south-western velocities. The different predictions of current amplitude were characterised by a slight tendency to overestimate observations. However, the complementary evaluation conducted in offshore waters confirmed model's performances. In the southern part of Ushant-Molène archipelago (point C3), predictions approached the pronounced asymmetry of tidal current components liable to reach $0.5\,\mathrm{m\,s^{-1}}$ in spring tidal conditions. An overall good agreement was also obtained in waters west of Ushant (point C4), both in current amplitude and direction, as exhibited by the associated values of NRMSE and the Pearson's correlation coefficients (Tab. 2).

Table 1: Description of current measurement campaigns considered.

Points	Coordinates		Water depths	Periods
	Lon.	Lat.	(m)	of measurements
C1	5.036° W	48.449° N	53	20/03/1993 → 02/04/1993
C2	4.945° W	48.423° N	29	17/05/1993 → 31/05/1993
C3	5.071° W	48.313° N	80	12/08/2012 → 23/08/2012
C4	5.403° W	48.496° N	110	26/02/2006 → 09/03/2006

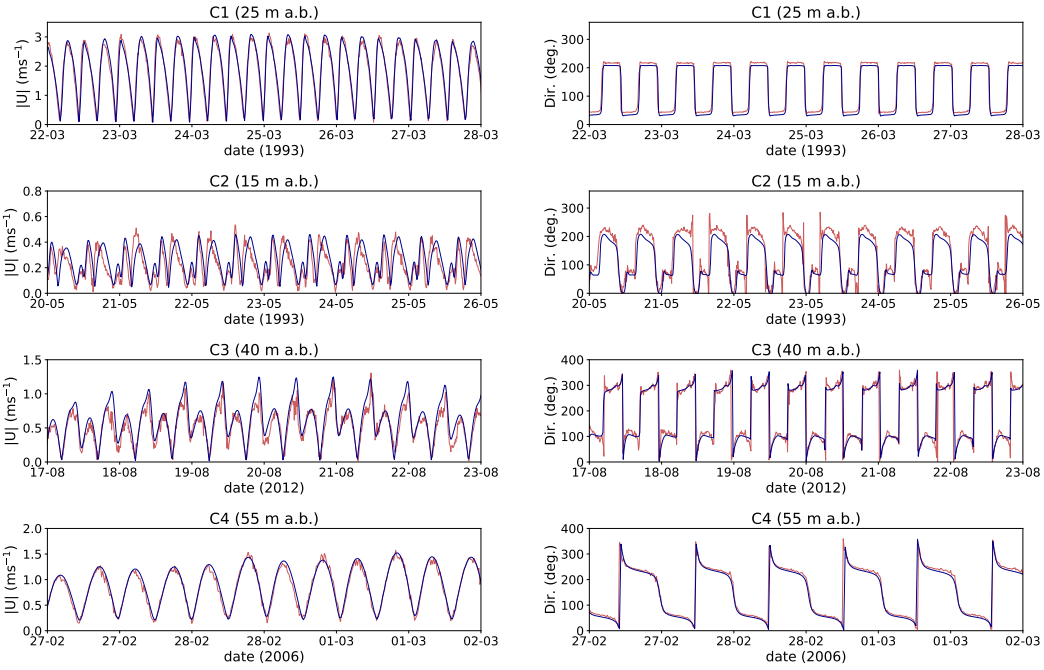

Figure 5: Measured (light red) and predicted (blue) time series of the amplitude and direction (anticlockwise convention from the east) of the current in mean-spring conditions and in mid-water depths at points C1, C2, C3 and C4.

Table 2: Statistical parameters for the evaluation of observed currents amplitude |U| and direction Dir at points C1-C4 during measurement campaigns: the mean relative difference $\mathrm{DIFF_{rel}}$, the Normalised Root-Mean-Square Error NRMSE and the Pearson's correlation coefficient R.

Measurement	|U|			Dir		
points	$\mathrm{DIFF_{rel}}$	NRMSE	R	$\mathrm{DIFF_{rel}}$	NRMSE	R
C1	$0.05\ \mathrm{m\,s^{-1}}$	14.1%	0.97	-8.7^{o}	16.4%	0.97
C2	$0.03\ \mathrm{m\,s^{-1}}$	46.6%	0.67	-19.4^{o}	29.7%	0.92
C3	$0.05\ \mathrm{m\,s^{-1}}$	28.9%	0.93	2.36^{o}	21.3%	0.91
C4	$0.04\ \mathrm{m\,s^{-1}}$	11.6%	0.99	-4.5^{o}	14.2%	0.97

4.2. Water renewal in the Ushant-Molène archipelago

4.2.1. Tracer concentration decay

The renewal of marine waters in the Ushant-Molène archipelago was investigated by (i) focusing on the spatial and temporal evolutions of tracer concentration and (ii) computing transport time descriptors within the control domain. However, in accordance with numerical assessments of water renewal in marine environments [47], the concentration of the neutrally-buoyant dye was characterised by semi-diurnal oscillations following the ebb and flood phases of the tidal cycle. As these oscillations may influence the evaluation of times concentration decay, values were averaged within the control domain and over $\mathrm{M_2}$ tidal cycles.

Rapid changes of the tracer concentration were obtained for initial releases in simulations a#1 to a#8 (Figs. 4 and 6). Half of the imposed concentration was thus lost in less than three days within the control domain (Tab. 3). It was furthermore estimated that a maximum of six days was required to evac-

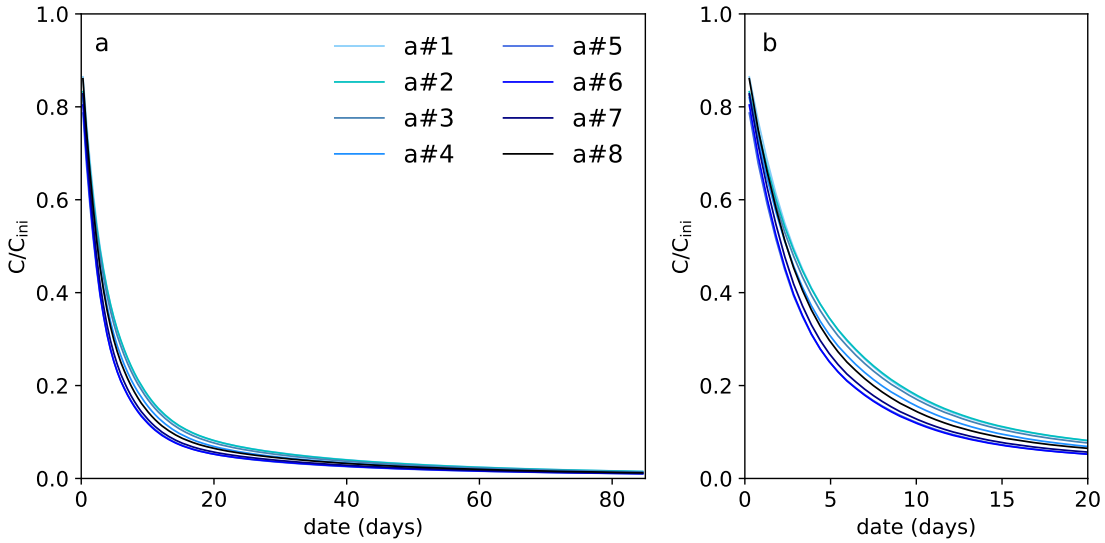

Figure 6: Tracer concentration decay, averaged within the control domain and over M_2 tidal cycles, in simulations a#1 to a#8 during (a) 85 and (b) 20 days.

Table 3: Mean (D_{mean}), minimum (D_{min}), and maximum (D_{max}) durations required for the averaged concentration within the control domain to decrease to 50, 30, 10, and 2% of the initial value for releases between times #a1 and #a8. Simulations were driven by M_2 and M_4. The fifth column displays the difference (in percentage of the mean duration) between the maximum and minimum durations $\Delta D = 100(D_{max} - D_{min})/D_{mean}$ while the last two columns indicate the times of tracer releases for D_{min} and D_{max}, respectively.

Percentiles of initial tracer concentration value	D_{mean} (days)	D_{min} (days)	D_{max} (days)	ΔD (%)	Time for D_{min}	Time for D_{max}
50%	2.4	1.9	2.8	36.6	a#5	a#1
30%	5.0	4.0	5.9	37.4	a#5	a#2
10%	14.0	11.5	16.5	36.3	a#6	a#2
2%	59.3	49.3	68.9	33.0	a#5	a#1

uate 70% of the initial concentration from the Ushant-Molène archipelago. Nevertheless, the tracer concentration was characterised by a residual value that decayed very slowly after 30 days of simulations. 2% of the initial tracer concentration was thus still present after 49 days, and over 1% was predicted after 85 days. This result was consistent with the numerical simulations conducted by Phelps et al. [47] in the hyper-tidal region of the Liverpool Bay (UK) indicating that the complete replenishment of the bay could take several years. Whereas further assessments of these predictions were required, these results confirmed also that the concentration decay could not be calibrated during the first days of simulation by simple exponential functions (Section 3.2.2). Differences existed furthermore for formulations (such as Murakami [52]) that gave weight to the long-term evolution (Fig. 3). As exhibited by Viero and Defina [40], the "1/e threshold" method, classically implemented in semi-enclosed basins, was thus found to underestimate the water renewal time in this marine area dominated by advection processes.

The simplified numerical approach, based on a depth-averaged tidal circulation model (Section 3), provided thus further insights about the renewal capacity of the Ushant-Molène archipelago and exposure of this marine ecosystem to biological or geochemical disturbances. The tidal energetic conditions of the area of interest will thus mitigate potential pollution problems with a rapid decrease of the tracer concentration. Particular attention should, however, be dedicated to residual concentrations whose values may exceed environmentally harmful levels.

4.2.2. Sensitivity to release time

Whereas the tidal phase was found to have a minor impact on water renewal in tidally-flushed semi-enclosed basins [40], more important effects were exhibited in the Ushant-Molène archipelago. Confirming the investigation conducted by Ascione Kenov et al. [56] at the Pertuis d'Antioche/Marennes-Oléron Bay (France), simulations a#1 to a#8 revealed a strong dispersion of renewal times in relation to the release time of tracer concentration during a M_2 tidal cycle. Differences were thus exhibited between the minimum and maximum durations (D_{min} and D_{max}) required for the averaged concentration (within the control domain) to decay until a given percentile of its initial value (Tab. 3). The associated relative variation, $\Delta D = 100(D_{max} - D_{min})/D_{mean}$, was estimated over 33% for the four percentiles estimations (50, 30, 10 and 2%). This represented a variation of nearly 20 days in the duration required for the averaged concentration to decay below 2% of its initial value. The highest durations of concentration decays were naturally obtained for initial releases in the vicinity of high tide (times a#1 and a#2, Fig. 4 and Tab. 3) as a more important amount of tracer mass was injected within the control domain. Conversely, minimum durations were predicted for tracer releases in the vicinity of low tides (times a#5 and a#6) when a reduced volume of tracer was initially prescribed. This prominent influence of the initial release time was confirmed by the evolution of the spatial distribution of tracer concentration in western Brittany (Fig. 7). The Ushant-Molène archipelago exhibited thus varying renewal capacity in relation to the tidal phase. It is therefore suggested that marine water quality studies in such tidally-dominated environments consider these

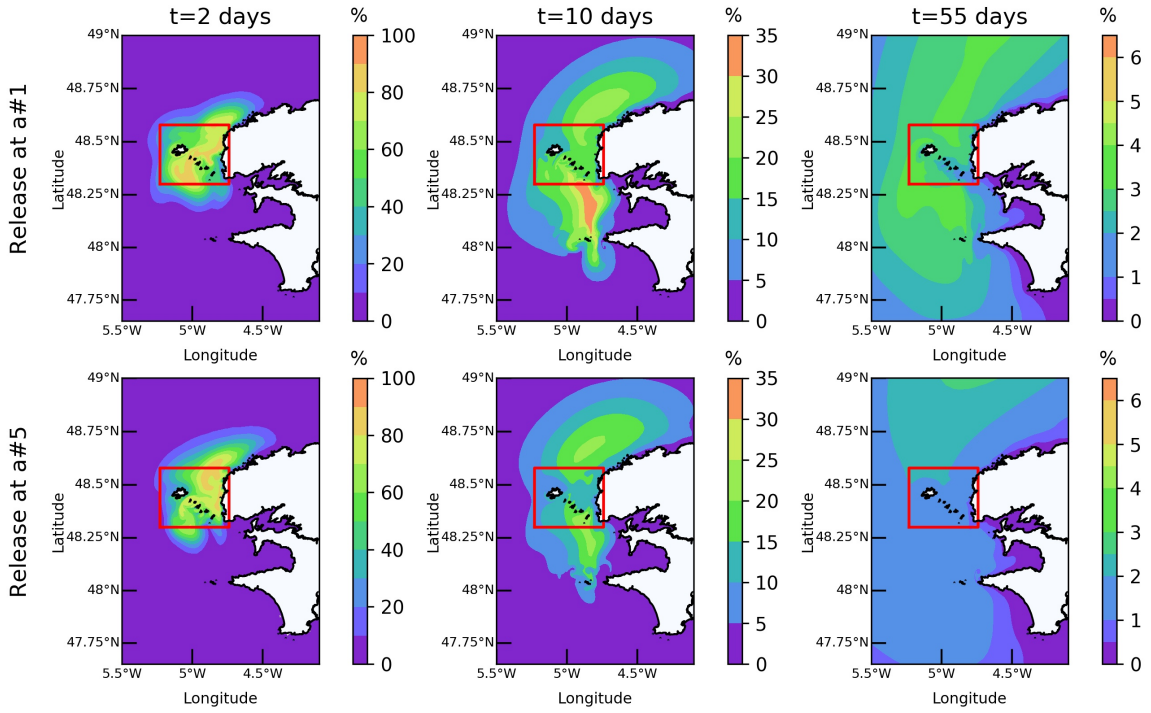

Figure 7: Spatial distributions of the tracer concentration (expressed in percentages of the initial value imposed within the control domain $C_{ini} = 1$) in simulations a#1 (high tide) and a#5 (low tide) of a M_2 tidal cycle after 2, 10 and 55 days. The red line delimits the area where tracer concentration is initially prescribed at $C_{ini} = 1$.

variations for a refined estimation of renewal capacities.

A close correlation was furthermore exhibited between the (i) spatial distribution of tracer concentration and (ii) the major features of circulation pathways predicted by Guillou and Chapalain [13, 14] (Section 2, Fig. 2). Predicted concentrations were thus following (i) the prominent north-eastern pathway and (ii) the southward circulation identified on both sides of the Fromveur Strait, resulting, after 10 days, in (i) one concentration cloud extending along the northern coast of western Brittany, and (ii) another one

spreading till the southern part of the island of Sein. These two areas of high concentration vanished after 50 days with a reduced impact within coastal basins of the bays of Brest and Douarnenez.

4.2.3. Sensitivity to spring-neap tidal conditions

In spring-neap tidal conditions (simulations b#1 to b#4), predicted tracer concentration decays were characterised by a stronger dispersion between D_{min} and D_{max} than in idealised M_2 and M_4 tidal forcing (simulations a#1 to a#8) (Tab. 4). These predictions were consistent with the simulation conducted by Uncles and Torres [57] in the Plymouth Sound (UK) that exhibited an increased variability of water flushing time scales with respect to spring-neap tidal conditions. Nevertheless, this variability slightly decayed after 10 days, as illustrated by the estimations of times required to fall below 10 and 2% of the initial concentration. Confirming the investigation in compound

Table 4: Mean (D_{mean}), minimum (D_{min}), and maximum (D_{max}) durations required for the averaged concentration within the control domain to decrease to 50, 30, 10, and 2% of the initial value for releases between times #b1 and #b4. Simulations were driven by M_2, M_4 and S_2. The fifth column displays the difference (in percentage of the mean duration) between the maximum and minimum durations $\Delta D = 100(D_{max} - D_{min})/D_{mean}$ while the last two columns indicate the times of tracer releases for D_{min} and D_{max}, respectively.

Percentiles of initial tracer concentration value	D_{mean} (days)	D_{min} (days)	D_{max} (days)	ΔD (%)	Time for D_{min}	Time for D_{max}
50%	2.4	1.2	3.3	89.0	b#1	b#4
30%	4.6	2.6	6.0	75.1	b#1	b#4
10%	12.5	10.4	15.3	39.2	b#1	b#2
2%	53.3	40.7	64.1	43.8	b#1	b#2

M_2-M_4 tide (Section 4.2.2), minimum durations were predicted for releases in low spring tides (simulation b#1). Maximum durations were obtained in simulations (i) b#2 with a high volume of tracer injected in spring tidal currents and (ii) b#4 with a reduced volume in neap tidal flow. Simulations driven by M_2 and M_4 provided increased estimations of the concentration decays (Tabs. 3 and 4). A relative consistency was, however, found between these simulations and simulations conducted in spring-neap tidal conditions. It was thus estimated that an average of 14 days was necessary to reach 10% of the initial concentration within the control domain in M_2-M_4 compound tide against 12.5 days in M_2-M_4-S_2. As simulations b#1 to b#4 only considered tracer releases in spring and neap tidal cycles, these differences may be reduced if an increased number of release times were considered in spring-neap tidal conditions. This result highlighted the relative consistency of the simplified M_2-M_4 tidal forcing for a preliminary evaluation of tracer concentration decay in north-western coastal waters of Brittany. Simulations a#1 to a#8 were thus retained to investigate the effects of tidal stream energy extraction on the renewal of marine water in the Ushant-Molène archipelago.

4.3. Effects of tidal stream energy extraction

The effects of tidal stream energy extraction were investigated for an array of 207 turbines adopting the configuration proposed by Thiébot et al. [17], with a density of 50 machines per km^2 over the area identified for the implementation of tidal stream arrays within the Fromveur Strait (Fig. 1). This energy extraction scenario was furthermore consistent with numerical investigations conducted by Guillou and Thiébot [18, 58] and Guillou and Chapalain [13, 14] in the area of interest. The integration of tidal stream tur-

bines slightly modified the residence time of tracer concentration within the Ushant-Molène archipelago with differences below 5.3% (Tab. 5). However, confirming previous numerical investigations performed within multi-inlet bay system [11], increased differences appeared locally on the spatial distributions of the tracer concentration. These local differences were exhibited in simulation a#1 characterised by the highest renewal times with more potential harmful environmental impacts of pollutants (Fig. 8). The predicted differences between the energy extraction scenario and the baseline configuration without turbines exhibited thus, in the early days of the simulation, increases of the tracer concentration in local areas, both upstream and downstream the Fromveur Strait. A close correlation was furthermore identified between the locations of (i) these retention areas and (ii) the cyclonic and anti-cyclonic residual eddies on both part of the strait (Fig. 2). This result

Table 5: Variations with turbines of mean (D_{mean}), minimum (D_{min}), and maximum (D_{max}) durations required for the averaged concentration within the control domain to decrease to 50, 30, 10, and 2% of the initial tracer value for initial releases between times #a1 and #a8 in the presence of tidal turbines. The last two columns indicate the times of tracer releases for D_{min} and D_{max} with turbines, respectively. Simulations were driven by M_2 and M_4.

Percentiles of initial tracer concentration value	δD_{mean} (%)	δD_{min} (%)	δD_{max} (%)	Time for D_{min}	Time for D_{max}
50%	+4.2	+5.3	+3.6	a#5	a#1
30%	+4.0	+5.0	+3.4	a#5	a#2
10%	+0.7	+1.7	+0.6	a#6	a#2
2%	-1.2	-1.2	-1.2	a#5	a#1

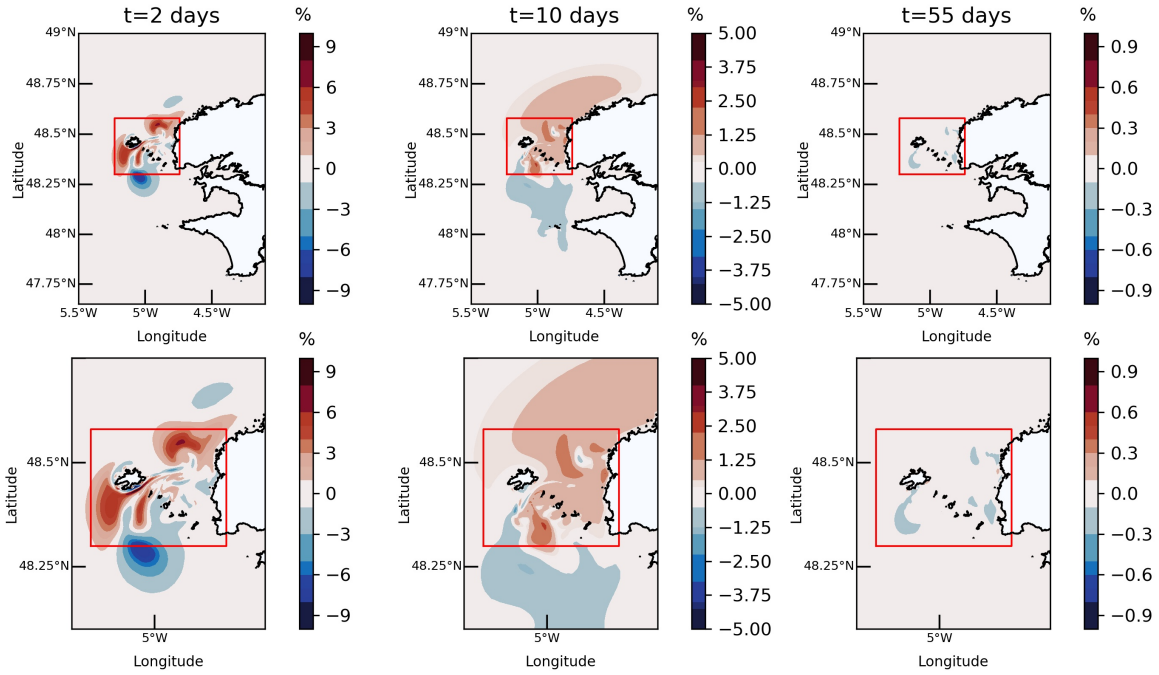

Figure 8: Spatial distributions of the differences in tracer concentration between the full energy extraction scenario and the baseline condition without turbines, in simulations a#1 after 2, 10 and 55 days. These differences are expressed in percentages of the initial concentration value imposed within the control domain $C_{ini} = 1$. The red line delimits the area where tracer concentration is initially prescribed at $C_{ini} = 1$.

was consistent with the numerical investigation performed by Guillou and Chapalain [13] on the residual Lagrangian circulation within the Ushant-Molène archipelago. Indeed, the extraction of tidal stream power was found to impact the locations of the south and north recirculations with a tendency for these features to get closer to the tidal stream energy site. Turbines' operation within this environment was thus liable to displace these eddies by more than 1.5 km increasing locally the tracer concentration on both parts of

the strait. However, this effect was superimposed on the increased transport of tracers associated with the development of two acceleration areas on the sides of the flow passing the farm location [18]. This effect was particularly noticeable after two days of simulations resulting in an increase of concentrations in the southern part of the strait. The reduction of tidal currents both upstream and downstream the tidal farm restricted furthermore the extension of the concentration cloud in the southern limit of the release zone with a decrease in tracer concentration. After 10 days of simulations, the extraction of tidal stream energy was found to slightly increase the tracer concentration in the northern part of western Brittany while decreasing the concentration in its southern part. Nevertheless, differences between simulations with and without turbines vanished after 55 days being restricted to values below 1% of the tracer concentration initially imposed within the control domain.

5. Conclusions

The depth-averaged circulation model Telemac 2D was implemented in the area surrounding the tidal stream energy site of the Fromveur Strait in western Brittany (France) to investigate the effects of turbines on the renewal of marine water. Numerical predictions were assessed against available in-situ observations of tidal currents amplitude and direction at four locations within the area of interest. Water renewal was estimated by (i) simulating the spatio-temporal evolution of a tracer concentration in idealised tidal forcings and (ii) computing the associated time of concentration decays within the Ushant-Molène archipelago. Sensitivities of these numerical estimations to the integration of turbines were investigated by simulating the far-field effects

of tidal stream energy extraction scenario of a full array with a simple equivalent drag force approach. The main outcomes of the present investigation are as follows:

1. Whereas simulations revealed a rapid decrease of the initial concentration with a 70% loss after six days, the tracer concentration decayed very slowly on longer time period with a residual value of 2% being still present after 85 days. This result confirmed, in particular, that the concentration decay could not be calibrated by simple exponential functions and that the "1/e threshold" method, traditionally implemented in bays and estuaries, could not be applied to these energetic marine environments.
2. The numerical estimations of concentration decays were furthermore characterised by a strong dispersion depending on the time of tracer releases during semi-diurnal and spring-neap time scales. In M_2-M_4 compound tide, a relative difference of more than 33% was thus found between the maximum and minimum durations required for the averaged concentration (within the control domain) to decay until a given percentile of its initial value.
3. The highest durations of concentration decays were mainly obtained for initial releases in the vicinity of high tide that corresponded to more significant amount of tracer mass within the area surrounding the Ushant-Molène archipelago.
4. Whereas a full energy extraction scenario was considered (with an array covering the area identified for the implementation of tidal farm and a constant thrust coefficient that extracted energy for the wide

range of tidal currents amplitudes), simulations exhibited weak effects of turbines on the time concentration decay within the control domain. The residence time of tracer concentration was thus modified by less than 5.3%. Local trapping areas were, however, identified in the early days following tracer concentration releases. The associated synoptic distribution was furthermore consistent with Lagrangian residual patterns computed from floats particles trajectories. The effects of tidal turbines vanished after 55 days.

This numerical study provided thus further insights about the renewal of marine water in the tidal stream energy site of the Fromveur Strait and the biosphere reserve of the Sea of Iroise. This first preliminary assessment of potential effects of a turbine array was important in such marine environment with high primary productivity and associated marine life. The simplified Eulerian approach based on transport of solute quantities complemented, in particular, the Lagrangian simulations of particles trajectories with a refined estimation of water renewal times. Complementary modelling of passive tracer transport (such as temperature or salinity) may be conducted to assess model's performances at extended spatial and temporal time scales. These refined simulations will require the implementation of a three-dimensional model that incorporates meteorological forcings (including wind and waves) and thermal stratification effects. Advanced representation of individual turbines (integrating the form drag of supporting structure and different hub heights along the water column) such as the actuator disk theory may also be considered. These refined numerical applications will finally help to encompass the seasonal and inter-annual variability of water transport and

associated renewal timescales in these energetic locations.

Acknowledgements

In-situ observations and bathymetric data used here were provided by the French navy SHOM ("Service Hydrographique et Océanographique de la Marine"). Numerical simulations were conducted on HPC facilities DATARMOR of "Pôle de Calcul et de Données pour la Mer" (PCDM) (http://www.ifremer.fr/pcdm). The present paper is a contribution to the research program DIADEME ("Design et InterActions des Dispositifs d'extraction d'Energie Marine avec l'Environnement") of the Laboratory of Coastal Engineering and Environment (Cerema, http://www.cerema.fr).

References

[1] D. Magagna, A. Uihlein, Ocean energy development in Europe: Current status and future perspectives, International Journal of Marine Energy 11 (2015) 84–104.

[2] R. Loisel, L. Lemiale, Comparative energy scenarios: Solving the capacity sizing problem on the French Atlantic Island of Yeu, Renewable and Sustainable Energy Reviews 88 (2018) 54–67.

[3] J. Van Der Molen, S. Rogers, J. Ellis, C. Fox, P. McCloghrie, Dispersal patterns of the eggs and larvae of spring-spawning fish in the Irish Sea, UK, Journal of Sea research (58) (2007) 313–330.

[4] M. Kadiri, R. Ahmadian, B. Bockelmann-Evans, W. Rauen, R. Falconer,

A review of the potential water quality impacts of tidal renewable energy systems, Renewable and Sustainable Energy Review 16 (2012) 329–341.

[5] S. Nash, A. Phoenix, A review of the current understanding of the hydro-environmental impacts of energy removal by tidal turbines, Renewable and Sustainable Energy Reviews 80 (2017) 648–662.

[6] J. Van Der Molen, P. Ruardij, N. Greenwood, Potential environmental impact of tidal energy extraction in the Pentland Firth at large spatial scales: Results of a biogeochemical model, Biogeosciences Discussions 12 (24) (2015) 20475–20514.

[7] M. De Dominicis, R. O'Hara Murray, J. Wolf, Multi-scale ocean response to a large tidal stream turbine array, Renewable Energy 114 (2017) 1160–1179.

[8] Z. Yang, T. Wang, Effects of Tidal Sream Energy Extraction on Water Exchange and Transport Timescales, in: Z. Yang, A. Copping (Eds.), Marine Renewable Energy, 259–278, 2017.

[9] Z. Yang, T. Wang, A. Copping, Modeling tidal stream energy extraction and its effects on transport processes in a tidal channel and bay system using a three-dimensional coastal ocean model, Renewable Energy 50 (2013) 605–613.

[10] S. Nash, N. O'Brien, A. Olbert, M. Harnett, Modelling the far field hydro-environmental impacts of tidal farms - A focus on tidal regime, inter-tidal zones and flushing, Computers & Geosciences 71 (2014) 20–27.

[11] T. Wang, Z. Yang, A modeling study of tidal energy extraction and the associated impact on tidal circulation in a multi-inlet bay system of Puget Sound, Renewable Energy 114 (2017) 204–214.

[12] G. I. Shapiro, Effect of tidal stream power generation on the region-wide circulation in a shallow sea, Ocean Sciences 7 (2011) 165–174.

[13] N. Guillou, G. Chapalain, Assessing the impact of tidal stream energy extraction on the Lagrangian circulation, Applied Energy 203 (2017) 321–332.

[14] N. Guillou, G. Chapalain, Evaluating the Effects of Tidal Turbines on Water-Mass Transport with the Lagrangian Barycentric Method, in: Proceedings of the Sixth International Conference on Estuaries and Coasts, Caen, France, 2018.

[15] S. Neill, J. Jordan, S. Couch, Impact of tidal energy convertor (TEC) arrays on the dynamics of headland sand banks, Renewable Energy 37 (2012) 387–397.

[16] D. Plew, C. Stevens, Numerical modelling of the effects of turbines on currents in a tidal channel - Tory Channel, New Zealand, Renewable Energy 57 (2013) 269–282.

[17] J. Thiébot, P. Bailly du Bois, S. Guillou, Numerical modeling of the effect of tidal stream turbines on the hydrodynamics and the sediment transport - Application to the Alderney Race (Raz Blanchard), France, Renewable Energy 75 (2015) 356–365.

[18] N. Guillou, J. Thiébot, The impact of seabed rock roughness on tidal stream power extraction, Energy 112 (2016) 762–773.

[19] C. Chen, H. Huang, R. C. Beardsley, Q. Xu, R. Limeburner, G. W. Cowles, Y. Sun, J. Qi, H. Lin, Tidal dynamics in the Gulf of Maine and New England Shelf: An application of FVCOM, Journal of Geophysical Research: Oceans 116 (C12010).

[20] S. Neill, M. Hashemi, M. Lewis, The role of tidal asymmetry in characterizing the tidal energy resource of Orkney, Renewable Energy 68 (2014) 337–350.

[21] N. Guillou, G. Chapalain, Tidal Turbines' Layout in a Stream with Asymmetry and Misalignment, Energies 10 (11) (2017) 1892.

[22] T. Roc, D. Conley, D. Greaves, Methodology for tidal turbine representation in ocean circulation model, Renewable Energy 51 (2013) 448–464.

[23] A. Goward-Brown, S. Neill, M. Lewis, Tidal energy extraction in three-dimensional ocean models, Renewable Energy 114 (2017) 1–17.

[24] SHOM, Courants de marée - Mer d'Iroise de l'île Vierge à la pointe de Penmarc'h, Technical Report 560-UJA, Service Hydrographique et Océanographique de la Marine, 2016.

[25] N. Guillou, S. P. Neill, P. E. Robins, Characterising the tidal stream power resource around France using a high-resolution harmonic database, Renewable Energy 123 (2018) 706–718.

[26] N. Guillou, G. Chapalain, S. P. Neill, The influence of waves on the tidal kinetic energy resource at a tidal stream energy site, Applied Energy 180 (2016) 402–415.

[27] J. C. Allo, Marine current energy for islands, in: Proceedings of IRENA - Martinique conference on island energy transitions, Martinique, 2015.

[28] N. Guillou, Modelling effects of tidal currents on waves at a tidal stream energy site, Renewable Energy 114 (2017) 180–190.

[29] J. M. Hervouet, Hydrodynamics of free surface flows, modelling with the finite element method, Cambridge University Press, Cambridge, 2007.

[30] A. Hamdi, M. Vasquez, J. Populus, Cartographie des habitats physiques Eunis - Côtes de France, Technical Report DYNECO/AG/10-26/JP, Ifremer, 2010.

[31] R. Soulsby, The bottom boundary layer of shelf seas, in: B. E. Johns (Ed.), Physical Oceanography of Coastal and Shelf Seas, Elsevier, Amsterdam, 189–266, 1983.

[32] N. Guillou, G. Chapalain, Numerical modelling of nearshore wave energy resource in the Sea of Iroise, Renewable Energy 83 (2015) 942–953.

[33] N. Guillou, Evaluation of wave energy potential in the Sea of Iroise with two spectral models, Ocean Engineering 106 (2015) 141–151.

[34] M. Hashemi, S. Neill, P. Robins, A. Davies, M. Lewis, Effect of waves on the tidal energy resource at a planned tidal stream array, Renewable Energy 75 (2015) 626–639.

[35] N. Guillou, G. Chapalain, E. Duvieilbourg, Modelling impact of bottom roughness on sea surface temperature in the Sea of Iroise, Continental Shelf Research 54 (2013) 80–92.

[36] N. Guillou, G. Chapalain, E. Duvieilbourg, Sea surface temperature modelling in the Sea of Iroise: assessment of boundary conditions, Ocean Dynamics 63 (2013) 849–863.

[37] G. Egbert, A. Bennett, M. Foreman, TOPEX/POSEIDON tides estimated using a global inverse model, Journal of Geophysical Research 99 (1994) 24821–24852.

[38] T. Dabrowski, M. Hartnett, A. Olbert, Influence of seasonal circulation on flushing of the Irish Sea, Marine Pollution Bulletin 60 (2010) 748–758.

[39] J. Sun, B. Lin, K. Li, G. Jiang, A modelling study of residence time and exposure time in the Pearl River Estuary, China, Journal of Hydro-environment Research 8 (2014) 281–291.

[40] D. P. Viero, A. Defina, Water age, exposure time, and local flushing time in semi-enclosed, tidal basins with negligible freshwater inflow, Journal of Marine Systems 156 (2016) 16–29.

[41] R. Pingree, L. Maddock, The M_4 tide in the English Channel derived from a non-linear numerical model of the M_2 tide, Deep-Sea Research 25 (1978) 53–63.

[42] N. Guillou, G. Chapalain, Numerical simulation of tide-induced transport of heterogeneous sediments in the English Channel, Continental Shelf Research 30 (2010) 806–819.

[43] K. R. Dyer, Estuaries: A Physical Introduction, John Wiley & Sons, 1973.

[44] A. de Brauwere, B. de Brye, S. Blaise, E. Deleersnijder, Residence time, exposure time and connectivity in the Scheldt Estuary, Journal of Marine Systems 84 (2011) 85–95.

[45] J. F. Bárcena, A. García, A. G. Gómez, C. Álvarez, J. A. J. ad J. A. Revilla, Spatial and temporal flushing time approach in estuaries influenced by river and tide. An application in Suances Estuary (Northern Spain), Estuarine, Coastal and Shelf Science 112 (2012) 40–51.

[46] T. Dabrowski, M. Hartnett, A. Olbert, Determination of flushing characteristics of the Irish Sea: A spatial approach, Computers & Geosciences 45 (2012) 250–260.

[47] J. J. C. Phelps, J. A. Polton, A. J. Souza, L. A. Robinson, Hydrodynamic timescales in a hyper-tidal region of freshwater influence, Continental Shelf Research 63 (2013) 13–22.

[48] N. E. Monsen, J. E. Cloern, L. V. Lucas, S. G. Monismith, A comment on the used of flushing time, residence time, and age as transport time scales, Limnology and Oceanography 47 (2002) 1545–1553.

[49] E. J. M. Delhez, On the concept of exposure time, Continental Shelf Research 71 (2013) 27–36.

[50] H. Takeoka, Fundamental concepts of exchange and transport time scales in a coastal sea, Continental Shelf Research 3 (3) (1984) 322–326.

[51] M. L. Sámano, J. F. Bárcena, A. Garcia, A. G. Gómez, C. Álvarez, J. A. Revilla, Flushing time as a descriptor for heavily modified water bodies classification and management: application to the Huelva Harbour, Journal of Environmental Management 107 (2012) 37–44.

[52] K. Murakami, Tidal exchange mechanism in enclosed regions, in: Proceedings of the Second International Conference on Hydraulic Modelling of Coast Estuary and River Waters, vol. 2, 111–120, 1991.

[53] E. Fernandez-Rodriguez, T. J. Stallard, P. K. Stansby, Experimental study of extreme thrust on a tidal stream rotor due to turbulent flow and with opposing waves, Journal of Fluids and Structures 51 (2014) 354–361.

[54] C. Frost, C. Morris, A. Mason-Jones, D. O'Doherty, T. O'Doherty, The effect of tidal flow directionality on tidal turbine performance characteristics, Renewable Energy 78 (2015) 609–620.

[55] Z. Zhou, M. Benbouzid, J. F. Charpentier, F. Scuiller, T. Tang, Developments in large marine current turbine technologies - A review, Renewable and Sustainable Energy Reviews 71 (2017) 852–858.

[56] I. Ascione Kenov, F. Muttin, R. Campbell, R. Fernandes, F. Campuzano, F. Machado, G. Franz, R. Neves, Water fluxes and renewal rates at Pertuis d'Antioche/Marennes-Oléron Bay, France, Estuarine, Coastal and Shelf Science 167 (2015) 32–44.

[57] R. Uncles, R. Torres, Estimating dispersion and flushing time-scales in

a coastal zone: Application to the Plymouth area, Ocean & Coastal Management 72 (2013) 3–12.

[58] N. Guillou, J. Thiébot, Environmental impact of a tidal stream farm: predictions sensitivity to bottom roughness, in: 15èmes journées de l'hydrodynamique, 2016.